Applied Physics Letters

Voltage polarity manipulation of the magnetoresistance sign in organic spin valve devices

Cite as: Appl. Phys. Lett. **104**, 262402 (2014); https://doi.org/10.1063/1.4885770
Submitted: 25 March 2014 . Accepted: 17 June 2014 . Published Online: 30 June 2014

S. W. Jiang, B. B. Chen, P. Wang, Y. Zhou, Y. J. Shi, F. J. Yue, H. F. Ding, and D. Wu

Voltage polarity manipulation of the magnetoresistance sign in organic spin valve devices

S. W. Jiang, B. B. Chen, P. Wang, Y. Zhou, Y. J. Shi, F. J. Yue, H. F. Ding, and D. Wu[a)]
National Laboratory of Solid State Microstructures and Department of Physics, Nanjing University, 22 Hankou Road, Nanjing 210093, People's Republic of China

(Received 25 March 2014; accepted 17 June 2014; published online 30 June 2014)

The spin transport in organic spin valve (OSV) devices has been systematically investigated by inserting a low work function material Al between ferromagnetic electrode and organic layer. The resistance and current-voltage curve symmetry are dramatically altered as increasing Al thickness, indicating that an electron-unipolar OSV is obtained. Moreover, the magnetoresistance sign depends on the voltage polarity for certain Al thickness. We attribute this phenomenon to the Fermi and the lowest unoccupied molecular orbits energies of the two electrodes responding to the spin injection and detection, respectively. These findings provide a simple approach to control both the carrier type and the spin direction simultaneously. © *2014 AIP Publishing LLC*.
[http://dx.doi.org/10.1063/1.4885770]

Organic semiconductors (OSCs) are promising materials with intriguing properties, which are absent in inorganic semiconductor counterparts and can further extend the capabilities and possibilities of modern electronic and photonic devices.[1] Organic light-emitting diodes (OLEDs) have been commercialized and much wider applications, such as organic field effect transistors (OFETs) and organic solar cell, etc., are expected in near future. In addition to these applications based-on controlling the charges of the carriers, the control of the spin degree of freedom in OSCs has attracted great interest recently, primarily supported by the possibilities of enhancing functionality or the performance of organic electronic devices. A spin-polarized OLED (spin-OLED), of which the electroluminescence intensity is controlled by manipulating the spin of the injected carriers,[2] and a universal implication logic gate in one single organic device, which is functionalized by the combination of organic spin valve (OSV) effects with memristors,[3] are two remarkable examples. The advantage of utilizing spin in OSCs is that the spin relaxation time is very long in comparison with inorganic materials, originated from very weak spin-orbit and hyperfine interactions.[4,5] In order to develop useful organic devices based on spin-related phenomena, it is desirable to have the ability to manipulate spin injection and transport in a controlled manner. However, this issue is scarcely addressed.

The organic spintronic device structure usually consists of two ferromagnetic (FM) electrodes separated by a thin organic space layer.[2–7] The FM electrodes sever as the spin injector and detector, respectively. In addition to spin injection into OSCs, to operate a functional organic spintronic device, such as spin-OLEDs, it is essential to be able to control the injected carrier type.[2,5] The most conventional method is the choice of a low/high work function metal as an electron/hole injector. However, the work function of the typical FM materials, such as Co, Fe, and $La_{0.7}Sr_{0.3}MnO_3$ (LSMO), is high and in a limited range, around 4.6–5.0 eV,[6,8] presumably leading to hole injection only for most OSCs. Recently, it was reported that an inserting a thin LiF polar layer at FM/organic interface can change the dominant spin band for carrier extraction and consequently the sign change of the magnetoresistance (MR).[9] Due to the limitation of the electric dipole moment of the polar materials, the energy level shift is less than 1 eV, which is not high enough to alter the type of the injected carriers. Therefore, the carrier type manipulating of the spin polarized current is an important step to realize useful organic spintronic devices.

Here, we report on an injection of spin polarized electrons into Alq_3 by inserting a thin low work function material, Al, at interface. The device resistance and the symmetry of the current-voltage (*I-V*) characteristics change dramatically as increasing Al thickness, indicating the injected carrier type of electrons. In particular, we observe a controllable sign reversal of the MR effects upon switching the polarity of the bias voltage. We attribute this unusual MR sign reversal to the different energy levels responding to the spin injection and detection. These findings open up a possibility for the development of practical organic spintronic devices with the control of both the carrier type (hole or electron) and the sign of the spin (up or down) simultaneously.

A 50-nm-thick LSMO strip was grown on $SrTiO_3$ (001) substrates by pulsed laser deposition (PLD) with a shadow mask to define a proper size as the bottom electrode. In order to prevent a possible current leakage at the device edges, ~100 nm $SrTiO_3$ was epitaxially grown with a shadow mask by PLD to cover the edges of the LSMO strip. After annealed in oxygen at atmospheric pressure at 1050 °C for 6 h, the LSMO surface showed an atomically flat surface.[10] An Alq_3 film was thermally evaporated at room temperature with a deposition rate of 0.6 Å/s. Without breaking vacuum, a shadow mask was put on the sample to deposit Al by thermal evaporation. Then a 20-nm-thick Co film was deposited by indirect deposition method.[11] The obtained OSV devices were cross-bar geometry with active area ~0.2 mm × 0.2 mm. The transport measurements were carried out in four-point geometry and the magnetization was measured by a superconducting quantum interference device (SQUID).

[a)]Electronic mail: dwu@nju.edu.cn

In order to understand the influence of the Al interfacial layer on the carrier injection, the electrical transport measurements were performed on the OSVs with different Al thickness. Fig. 1(a) shows the typical current-voltage (*I-V*) characteristics measured at 10 K for LSMO/Alq_3 (30 nm)/Al (0–6 nm)/Co OSVs. The *I-V* curves for the OSVs without Al layer exhibit nearly symmetric behavior and low resistance at low voltage (<1 V), consistent with previous studies.[6] Although the low resistance level was frequently observed in many OSVs using other organic materials,[12,13] the comprehensive understanding is still not established. Recent ultraviolet photoelectron spectra (UPS) measurements showed that the deposition of Co on Alq_3 induced substantial intra-gap states between the highest occupied molecular orbits (HOMO) and lowest unoccupied molecular orbits (LUMO) levels.[14] The intra-gap states at the interface may provide small energy steps to facilitate current injection, resulting in a higher injecting current, similar as the electron injection at the indium tin oxide (ITO)/copper phthalocyanine (CuPc) interface.[15]

Once a thin Al layer inserts between Co and Alq_3, the *I-V* characteristics are dramatically altered, showing a strong impact of Al on carrier injection. The *I-V* curves become progressively more asymmetric as increasing the Al thickness and eventually a strong rectification behavior is observed with the rectification ratio of about 100 at ±4 V for 5 nm Al. Meanwhile, the resistance of the devices increases dramatically from a few kΩ to more than 100 MΩ at 0.2 V as increasing the Al thickness, shown in the inset of Fig. 1(a). Such large resistance at low voltage is frequently observed in the OLEDs involving Al/Alq_3 interfaces,[16] which is attributed to the penetration of Al into Alq_3 and the formation of the reacted states at interface.[17,18] The reacted interface states change the electronic properties and modify the charge injection properties of the interface. The Al layer may not only reduce the intra-gap states but also react with Alq_3, lead to the large resistance increment. As the Al thickness ~3 nm, Alq_3 layer is fully covered and hence the resistance becomes stable. At negative voltage, which means that the voltage of LSMO electrode is lower than that of the other electrode, the carriers could be holes injected from the Al/Co electrode to HOMO level and/or electrons injected from the LSMO electrode to LUMO level. Since Al is an electron injector for Alq_3 and the electron mobility in Alq_3 is one to two orders of magnitude higher than that of holes,[19,20] the hole injection from Al/Co electrode to Alq_3 is highly unlikely, particularly at low voltage range, implying that the carriers are only electrons injected from LSMO. If the voltage is reversed, the electrons are injected into Alq_3 from the Al/Co electrode and the holes injection from LSMO is unlikely. Therefore, unlike the type of the injected carriers under debate at Co/Alq_3 interface,[21,22] the carriers of the devices with Al layer are predominated by electrons. The highly asymmetric *I-V* curves suggest that the electron barrier height at Alq_3/Al interface is lower than at LSMO/Alq_3 interface.

Figure 1(b) shows that the saturation magnetization, M_S, is almost the same for 7 nm Co on Si/Alq_3 and Si/Alq_3/Al, in which Co was deposited simultaneously by indirect deposition. The smaller coercivity field for Si/Alq_3/Co sample may be due to the rougher Alq_3 surface. The blocking temperature, T_B, is well above 320 K for Si/Alq_3/Co sample from the zero field cooling (ZFC) and field cooling (FC) measurements, shown in the inset of Fig. 1(b). In contrast, M_S is significantly reduced and T_B is around 220 K for Co directly deposited on Alq_3 due to the interfacial interdiffusion.[23,24] These results suggest that the interdiffusion at interface is significantly suppressed using indirect deposition and Co clusters must be much larger with respect to directly deposited Co or may be eliminated.

Based on the above results that the carrier injection can be manipulated by the Al interfacial layer, it is interesting to study the spin transport in the electron-only devices. Fig. 2 shows the bias dependence of LSMO/Alq_3 (30 nm)/Co OSVs at 10 K, and the inset shows a typical MR curve measured at −0.1 V. The MR ratio is defined as $MR = (R_{AP} - R_P)/R_P$, where R_{AP} and R_P are the resistance of the magnetization of the LSMO and Co electrodes in the antiparallel and parallel configurations, respectively. The OSVs exhibit an inverse or

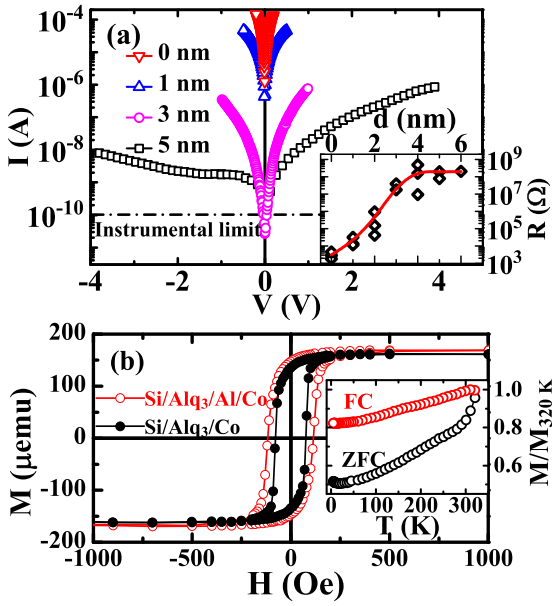

FIG. 1. (a) *I-V* curves for LSMO/Alq_3 (30 nm)/Al (0–5 nm)/Co OSVs with different Al thickness measured at 10 K. Inset: device resistance at 0.2 V as a function of Al thickness. The red line is a guide to the eyes. (b) Room temperature hysteresis loops for Si/Alq_3 (50 nm)/Co (7 nm) and Si/Alq_3 (50 nm)/Al (5 nm)/Co (7 nm), respectively. Inset: temperature dependence of the magnetization measured on Si/Alq_3 (50 nm)/Co (7 nm) (10 Oe in-plane magnetic field).

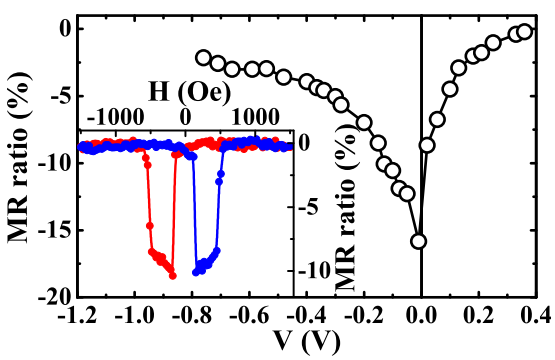

FIG. 2. MR ratio as a function of the bias voltage of LSMO/Alq_3 (30 nm)/Co OSVs measured at 10 K. Inset: MR loop measured at −0.1 V.

negative spin valve effect at all bias voltage and the maximum MR appears around zero voltage. These results, including that the MR ratio decays faster as increasing positive voltage than negative voltage, are consistent with previous reports.[6,13]

For the OSVs with very thin Al ($<\sim 2$ nm), of which the resistance is less than MΩ, we observe similar MR behaviors as the OSVs without Al, i.e., the inverse MR in all bias voltage and the MR ratio peaking at zero voltage. This is probably due to the Alq_3 layers are not fully covered by Al. Fig. 3(a) shows the surface morphology of 30 nm Alq_3 film grown on LSMO film, measured by *ex situ* atomic force microscopy. The root-mean-square roughness is typically ~1 nm. For the very thin Al films on Alq_3, the existence of pinholes in Al is very likely. At the region that Alq_3 is not covered, the LSMO/Alq_3/Co OSVs would be formed locally. Since the resistivity of LSMO/Alq_3/Co is several orders of magnitude smaller than that of LSMO/Alq_3/Al/Co, the pinhole regions would dominate the charge transport characteristics. Therefore, the performance of LSMO/Alq_3/Al ($<\sim 2$ nm)/Co OSVs is actually like that of LSMO/Alq_3/Co OSVs, but with much larger resistance. This is supported also by the temperature dependence of OSV resistance, shown in Fig. 3(b). For Al thinner than ~2 nm, the resistance slowly increases as decreasing temperature, similar as LSMO/Alq_3/Co.[6] In contrast, for Al thickness above ~2 nm, the resistance increases about two orders of magnitude as decreasing temperature to ~10 K, suggesting that ~2 nm is the critical thickness for Alq_3 fully covered by Al.

As the Al layer thickness increases above 2 nm, the characteristics of LSMO/Alq_3/Al/Co OSVs are entirely different from LSMO/Alq_3/Co OSVs. At negative voltage, the MR sign is inverted. Fig. 4(a) displays a typical inverted MR loop of LSMO/Alq_3 (30 nm)/Al (3 nm)/Co OSV measured at 10 K and −0.12 V. However, at positive voltage, the MR of the same device reverses its sign to positive, as represented by a typical MR loop measured at 0.12 V in Fig. 4(b). This peculiar phenomenon is more clearly seen in the plot of MR ratio as a function of voltage, shown in Fig. 4(c). The abrupt change of MR at zero voltage has never been observed in OSVs without an interfacial Al layer and inorganic magnetic tunnel junctions (MTJs). Similar as regular OSVs, the absolute value of MR ratio gradually decreases as increasing voltage. These results suggest that the Alq_3 layers are fully covered by Al and Al plays an important role in spin injection. Otherwise, a negative MR loop would be observed at positive voltage, like the OSVs without Al. We note that the

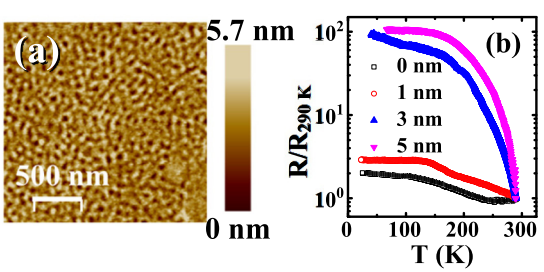

FIG. 3. (a) AFM image of 30 nm Alq_3 film grown on LSMO film. (b) Temperature dependence of resistance for LSMO/Alq_3 (30 nm)/Al (0–5 nm)/Co OSVs with different Al thickness measured at 0.2 V.

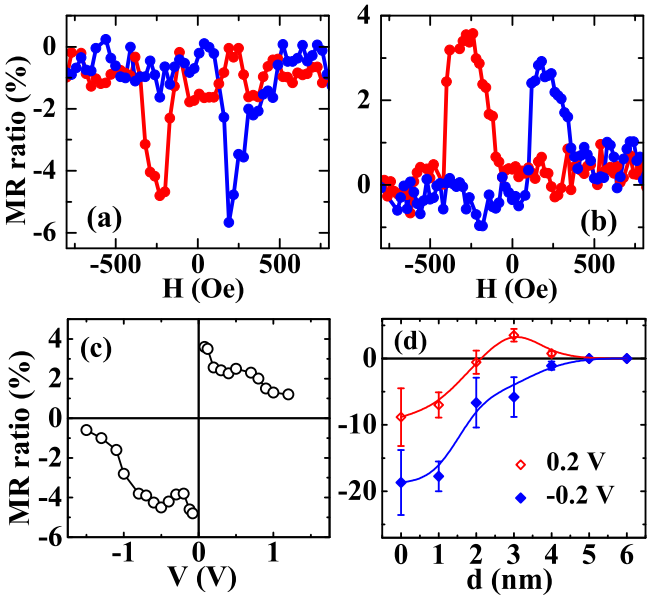

FIG. 4. MR loops of LSMO/Alq_3 (30 nm)/Al (3 nm)/Co OSV measured at 10 K with a bias voltages of (a) −0.12 V and (b) 0.12 V, respectively. (c) MR ratio as a function of the bias voltage for LSMO/Alq_3 (30 nm)/Al (3 nm)/Co OSVs. (d) MR ratio at 0.2 and −0.2 V, respectively, as a function of Al thickness. The lines are guide to the eyes.

MR ratio of the OSVs with Al is smaller than that of the OSVs without Al due to the reduced spin polarization as spin polarized current transport through Al. When the Al thickness is above 5 nm, the MR effects are not observed, as shown in Fig. 4(d), indicating the complete loss of the spin injection.

A recent theoretical calculation shows a MR sign reversal at ~0.25 V due to the molecular orbital localized in the electrical field direction in a single molecule device.[25] In our case, the electric field is ~0.03 V/nm at 1 V, which is too small to induce an observable change. Moreover, the electrode-molecule distance is critical for this effect, meaning that thermal fluctuation can easily smear out this effect.[25] This mechanism cannot explain our results.

The dependence of MR sign on the voltage polarity was shown in part of LSMO/Alq_3/Co samples, in which Co was directly deposited.[26] It was attributed to small Co clusters at interface acting as the counter electrode of LSMO and their magnetic switching different from Co film and uncontrollable. From above discussion, the interdiffusion at interface is largely suppressed and the size of Co clusters is relative large using indirect deposition, suggesting that Co clusters should not play significant role in MR. Indeed, we always observed negative MR in LSMO/Alq_3/Co OSVs using indirect deposition.[10,11] We fabricated several devices for each Al thickness. Although the resistance and MR ratio vary, the bias dependence characteristics are essentially the same.

The MR sign and MR ratio are usually estimated in terms of the Jullière formula: $MR = 2P_1P_2/(1 - P_1P_2)$, where P_1 and P_2 are the spin polarizations of the two FM electrodes.[27] The spin polarization is commonly accepted to be determined by the interaction between the states around Fermi energy, E_F, of FM electrodes and molecules (or insulators in MTJs) rather than FM electrodes alone.[28,29]

Therefore, it is possible to manipulate the spin polarization by engineering the interfacial interaction to obtain very large MR effects.[28] In any case, the spin polarization is an intrinsic property of the interface, implying that the MR sign cannot be changed via the polarity of the voltage.

Here, we propose a phenomenological model based on spin injection and detection at FM/Alq_3 interfaces to explain the MR sign reversal at zero voltage. Fig. 5 illustrates the energy diagrams of the LSMO/Alq_3/Al/Co OSVs with voltages, in which the carriers are dominated by electrons as discussed above. At negative voltage (Fig. 5(a)), electrons are injected from LSMO at E_F, transported through the Alq_3 LUMO energy and extracted by the Al/Co electrode. Since the electron extraction occurs at LUMO energy, the Co spin polarization at LUMO energy, which is about 0.5 eV above Al/Co E_F,[30] should be response to the spin polarized electron extraction.[9,31,32] It means that, according to Jullière formula, the positive spin polarization of LSMO at E_F and the negative spin polarization of Co at the Alq_3 LUMO energy would lead to negative MR. For positive voltage (Fig. 5(b)), we apply the same scenario, meaning that the MR sign is determined by the spin polarizations of Co at E_F and LSMO at the Alq_3 LUMO energy. According to X-ray photoemission spectroscopy measurements, the Alq_3 LUMO energy is about 1.26 eV above LSMO E_F.[8] A recent theoretical calculations show that the spin-down density of states (DOS) is higher than the spin-up DOS above $E_F \sim 1$ eV for LSMO, indicating the negative spin polarization at LUMO energy.[33] Therefore, considering the negative spin polarization of Co at E_F, a positive MR is expected at positive voltage.

In conclusion, we have experimentally demonstrated the electrical control of the MR sign by the polarity of the bias voltage in LSMO/Alq_3/Al/Co OSVs. This control can be understood by a proposed phenomenological model, of which spin polarization at the Fermi and LUMO energies of the electrodes is response to the spin injection and extraction, respectively, for electrons. These results show that the carrier type can be tuned by adding an ultrathin Al interfacial layer. Our approach can be extended to manipulate the carrier type, either electrons or hole, and spin type, either spin-up or spin-down, simultaneously by the introduction of an ultrathin non-FM metal. It provides us more flexibility to explore fundamental understanding and realize useful OSV devices.

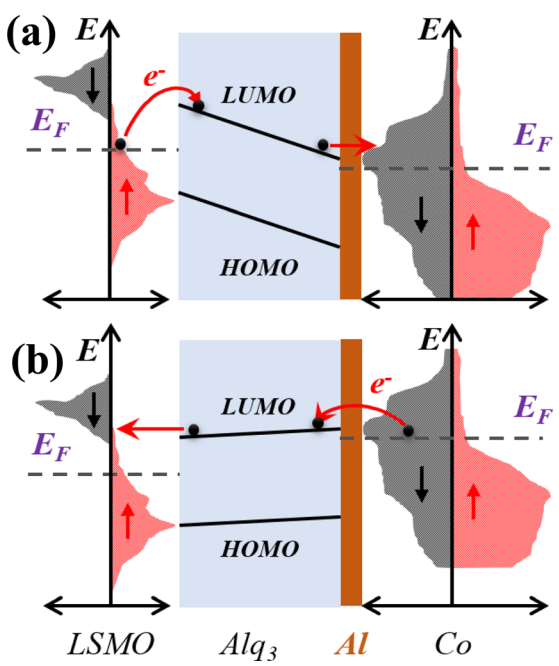

FIG. 5. The energy-level diagrams of LSMO/Alq_3/Al/Co with (a) a negative bias voltage and (b) a positive bias voltage.

We thank Y. Song for SQUID measurements and J. Du for helpful discussion. This work was supported by National Basic Research Program of China (Nos. 2010CB923402 and 2013CB922103), NSF of China (Nos. 11222435 and 11023002), NSF of Jiangsu Province (BK20130054).

[1]R. H. Friend, R. W. Gymer, A. B. Holmes, J. H. Burroughes, R. N. Marks, C. Taliani, D. D. C. Bradley, D. A. Dos Santos, J. L. Bredas, M. Lögdlund, and W. R. Salaneck, Nature **397**, 121 (1999).
[2]T. D. Nguyen, E. Ehrenfreund, and Z. V. Vardeny, Science **337**, 204 (2012).
[3]M. Prezioso, A. Riminucci, P. Graziosi, I. Bergenti, R. Rakshit, R. Cecchini, A. Vianelli, F. Borgatti, N. Haag, M. Willis, A. J. Drew, W. P. Gillin, and V. A. Dediu, Adv. Mater. **25**, 534 (2013).
[4]G. Szulczewski, S. Sanvito, and M. Coey, Nat. Mater. **8**, 693 (2009).
[5]V. A. Dediu, L. E. Hueso, I. Bergenti, and C. Taliani, Nat. Mater. **8**, 707 (2009).
[6]Z. H. Xiong, D. Wu, Z. V. Vardeny, and J. Shi, Nature **427**, 821 (2004).
[7]D. Sun, L. Yin, C. Sun, H. Guo, Z. Gai, X.-G. Zhang, T. Z. Ward, Z. Cheng, and J. Shen, Phys. Rev. Lett. **104**, 236602 (2010).
[8]Y. Q. Zhan, I. Bergenti, L. E. Hueso, V. Dediu, M. P. de Jong, and Z. S. Li, Phys. Rev. B **76**, 045406 (2007).
[9]L. Schulz, L. Nuccio, M. Willis, P. Desai, P. Shakya, T. Kreouzis, V. K. Malik, C. Bernhard, F. L. Pratt, N. A. Morley, A. Suter, G. J. Nieuwenhuys, T. Prokscha, E. Morenzoni, W. P. Gillin, and A. J. Drew, Nat. Mater. **10**, 39 (2011).
[10]B. B. Chen, Y. Zhou, S. Wang, Y. J. Shi, H. F. Ding, and D. Wu, Appl. Phys. Lett. **103**, 072402 (2013).
[11]S. Wang, Y. J. Shi, L. Lin, B. B. Chen, F. J. Yue, J. Du, H. F. Ding, F. M. Zhang, and D. Wu, Synth. Met. **161**, 1738 (2011).
[12]Y. Liu, S. M. Watson, T. Lee, J. M. Gorham, H. E. Katz, J. A. Borchers, H. D. Fairbrother, and D. H. Reich, Phys. Rev. B **79**, 075312 (2009).
[13]F. J. Wang, C. G. Yang, Z. V. Vardeny, and X. G. Li, Phys. Rev. B **75**, 245324 (2007).
[14]W. Xu, J. Brauer, G. Szulczewski, M. S. Driver, and A. N. Caruso, Appl. Phys. Lett. **94**, 233302 (2009).
[15]G. Parthasarathy, P. E. Burrows, V. Khalfin, V. G. Kozlov, and S. R. Forrest, Appl. Phys. Lett. **72**, 2138 (1998).
[16]T. D. Nguyen, Y. Sheng, J. Rybicki, and M. Wohlgenannt, Phys. Rev. B **77**, 235209 (2008).
[17]J. H. Lee, Y. Yi, and D. W. Moon, Appl. Phys. Lett. **93**, 153307 (2008).
[18]M. G. Mason, C. W. Tang, L.-S. Hung, P. Raychaudhuri, J. Madathil, D. J. Giesen, L. Yan, Q. T. Le, Y. Gao, S.-T. Lee, L. S. Liao, L. F. Cheng, W. R. Salaneck, D. A. dos Santos, and J. L. Brédas, J. Appl. Phys. **89**, 2756 (2001).
[19]C. L. Yang, Z. K. Tang, W. K. Ge, J. N. Wang, Z. L. Zhang, and X. Y. Jian, Appl. Phys. Lett. **83**, 1737 (2003).
[20]T. Sakanoue, M. Yahiro, C. Adachi, K. Takimiya, and A. Toshimitsu, J. Appl. Phys. **103**, 094509 (2008).
[21]Y. Q. Zhan, M. P. De Jong, F. H. Li, V. Dediu, M. Fahlman, and W. R. Salaneck, Phys. Rev. B **78**, 045208 (2008).
[22]J. S. Jiang, J. E. Pearson, and S. D. Bader, Phys. Rev. Lett. **106**, 156807 (2011).
[23]A. A. Sidorenko, C. Pernechele, P. Lupo, M. Ghidini, M. Solzi, R. De Renzi, I. Bergenti, P. Graziosi, V. Dediu, L. Hueso, and A. T. Hindmarch, Appl. Phys. Lett. **97**, 162509 (2010).

[24]C. Pernechele, I. Bergenti, M. Solzi, M. Ghidini, F. Casoli, and V. Dediu, J. Magn. Magn. Mater. **322**, 1251 (2010).
[25]S. Mandal and R. Pati, ACS Nano **6**, 3580 (2012).
[26]H. Vinzelberg, J. Schumann, D. Elefant, R. B. Gangineni, J. Thomas, and B. Büchner, J. Appl. Phys. **103**, 093720 (2008).
[27]M. Julliere, Phys. Lett. A **54**, 225 (1975).
[28]C. Barraud, P. Seneor, R. Mattana, S. Fusil, K. Bouzehouane, C. Deranlot, P. Graziosi, L. Hueso, I. Bergenti, V. Dediu, F. Petroff, and A. Fert, Nat. Phys. **6**, 615 (2010).
[29]A. Fert, Rev. Mod. Phys. **80**, 1517 (2008).
[30]L. Yan, M. G. Mason, C. W. Tang, and Y. Gao, Appl. Surf. Sci. **175**, 412 (2001).
[31]D. Sun, M. Fang, X. Xu, L. Jiang, H. Guo, Y. Wang, W. Yang, L. Yin, P. C. Snijders, T. Z. Ward, Z. Gai, X.-G. Zhang, H. N. Lee, and J. Shen, e-print arXiv:1304.2446.
[32]V. Dediu, L. E. Hueso, I. Bergenti, A. Riminucci, F. Borgatti, P. Graziosi, C. Newby, F. Casoli, M. P. De Jong, C. Taliani, and Y. Zhan, Phys. Rev. B **78**, 115203 (2008).
[33]J. M. Pruneda, V. Ferrari, R. Rurali, P. B. Littlewood, N. A. Spaldin, and E. Artacho, Phys. Rev. Lett. **99**, 226101 (2007).